

Highly Luminescent Gels and Mesogens Based on Elaborated Borondipyrromethenes

Franck Camerel,[†] Laure Bonardi,[†] Marc Schmutz,[‡] and Raymond Ziessel^{*†}

Laboratoire de Chimie Moléculaire (LCM), associé au CNRS, ULP-ECPM, 25 rue Becquerel, 67087 Strasbourg, France, and Institut Charles Sadron, CNRS, UPR 22, 6 rue Boussingault, 67083 Strasbourg, France

Received January 26, 2006; E-mail: ziessel@chimie.u-strasbg.fr

Supramolecular gels¹ and liquid crystalline materials² are fascinating organized soft materials that can respond to external stimuli such as heat, electrical pulses, light, and chemicals. Gelation properties can also be reversibly switched by changes in pH, geometry, or oxidation state.³ Particularly challenging is the use of gels in colorimetric sensing, electrooptical devices (fast response display), photovoltaic devices (light harvester), and as templates for the preparation of nanoporous materials and for assembling nanoparticles.¹ Recently, they have been used in biomedical applications for the controlled release of molecules, specifically for drug delivery.⁴

Our interests in luminescent organogels and discotic architectures based on metal complexes led us to synthesize supramolecular amphiphilic materials from long-chain alkoxydiacylamido platforms bearing chelating oligopyridine cores, these being able to self-assemble into columnar mesophases or fibrous networks by means of intermolecular hydrogen bonds.⁵ Unfortunately, they did not prove to form highly luminescent transition metal ion derivatives, and in all cases the gelation and LC properties were also suppressed. This caused us to consider replacement of metallic luminophores by purely organic fluorophores, provided those with appropriate properties such as ease of synthesis, stability, and high luminescence quantum yields could be found. Promising materials appeared to be the class of 4,4-difluoro-4-bora-3a,4a-diaza-*s*-indacene (*F*-Bodipy) derivatives.⁶ These molecules exhibit remarkable optoelectronic properties, with strong absorption in the visible region, high fluorescence quantum yields, and narrow emission bandwidths with high peak intensities. Herein we describe a new class of highly fluorescent mesomorphic dyes and gelators based on *F*-Bodipy that exhibit reversible phase transitions, in solid state, detectable by fluorescence spectroscopy.

The present system features a *F*-Bodipy unit tethered to a central 3,5-diacylamidotoluene platform equipped with two lateral aromatic rings each bearing three appended aliphatic chains. The methyl substituent of the central ring of the platform is essential to tilt the adjacent amide units out of the ring plane and thus favor intermolecular H-bonding, while meso substitution produces minimal inhibition of its tendency to π -stack in the solid state. The preparation of **1** (74% isolated yield) involves the reaction of the 4-carboxylic acid-3,5-diacylamidotoluene and 4-aminophenyl-Bodipy by means of EDC·HCl and DMAP.

Compound **1** displays two transitions centered at 213.7 °C ($\Delta H = 11.9 \text{ kJ}\cdot\text{mol}^{-1}$) and 25.1 °C ($\Delta H = 113.3 \text{ kJ}\cdot\text{mol}^{-1}$), on the cooling DSC curve. Cooling from the isotropic liquid, the fluid material becomes birefringent as observed by polarized optical microscopy (POM) and pseudo-fan-shaped textures with large homeotropic domains, typical of columnar mesophases, are observed under polarized light (Figure 2a).

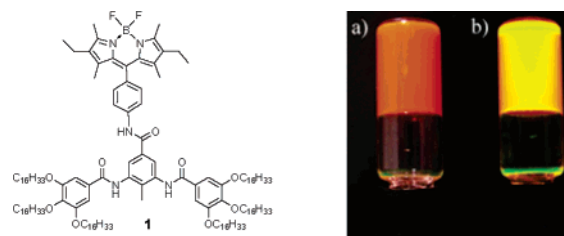


Figure 1. (a) Gelation test in nonane (22 g L⁻¹). Minimum gel concentration) = 16 g L⁻¹. Gel formation is confirmed if the sample does not flow in a few hours after the test tube is turned upside down. (b) Same gel observed upon UV irradiation at 356 nm.

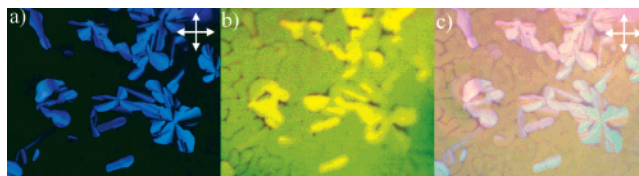


Figure 2. Compound **1** observed at 212 °C: (a) by POM with white light transmitted between crossed-polarizers (symbolized by the cross in the corner), (b) by fluorescence microscopy upon excitation at 300–350 nm without polarizer, (c) by superimposition of the texture observed by transmission in (a) and the texture observed by fluorescence in (b).

The luminescence properties of **1** in the mesophase and in the isotropic melt were studied using a fluorescence microscope equipped with a heating stage. In its isotropic state (>217 °C), the luminescence appears yellow-green and uniform as would be expected from randomly distributed molecules. However, in the mesophase, brightly luminescent pseudo-fan shapes are observed without any polarizer (Figure 2b), correlating with the texture observed by POM (Figure 2c). During the transition from the mesophase to the crystalline state at 28 °C, a global color change is observed by fluorescence from yellow-green to orange-red and is attributed to the formation of aggregates (vide infra), leading to a bathochromic shift of the emitted light. This is the first time that the texture of a thermotropic liquid crystal based on an *F*-Bodipy framework has been observed by fluorescence emission.

The presence of three amide tethers on the amphiphilic molecule **1** and the formation of columnar aggregates in the mesomorphic state prompted us to probe its gelation ability. Heating **1** in linear alkane chain solvents gives homogeneous, fluid solutions that provide robust gels on cooling. Upon UV irradiation at 356 nm, these gels appear highly fluorescent (Figure 1). DSC measurements performed on a gel at 22 g L⁻¹ showed a single reversible sol/gel transition centered at 48.5 °C ($\Delta H = 0.53 \text{ kJ mol}^{-1}$) on the heating curves and a reverse process at 27.3 °C (Figure S1). FT-IR spectra obtained on a gel at 31 g L⁻¹ in nonane exhibit single ν_{CO} and ν_{NH} , stretching vibrations, respectively, at 1647 and 3287 cm⁻¹, typical of amides engaged in a hydrogen-bonding network.⁷ Variable-temperature FT-IR spectroscopy shows that the gel/sol

[†] LCM.

[‡] Institut Charles Sadron.

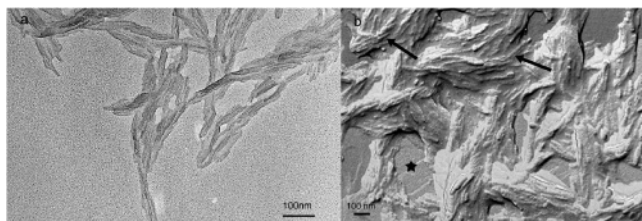


Figure 3. (a) Image obtained by TEM of a diluted gel of **1** in nonane ($c = 0.27 \text{ g L}^{-1}$). This observation was performed after rotary shadowing of the adsorbed solution onto a carbon coated grid. (b) Interconnected fibrils (arrows) observed by FFEM in a gel of **1** in nonane ($C = 27.5 \text{ g L}^{-1}$). (★) Corresponds to the crystallization of the nonane.

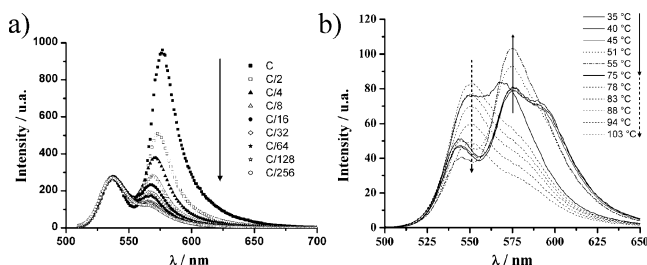


Figure 4. (a) Normalized emission spectra at 537 nm of **2** in nonane at different concentrations ($C = 3.6 \times 10^{-5} \text{ mol L}^{-1}$). (b) Temperature-dependent emission spectra of a gel from **2** at 22 g L^{-1} in nonane. Excitation wavelength = 490 nm.

transition observed above $48 \text{ }^\circ\text{C}$ does not result in disruption of the hydrogen-bonded network. ^1H and ^{11}B NMR spectra obtained in the gel state confirm that the resonance signals are dampened by motional broadening, indicating that gelation is due to the aggregation of the molecules into large objects.

TEM experiments were performed to examine the morphology of these gel materials and the nature of the aggregated objects that induce the gelation. Images obtained from diluted solutions in nonane reveal the presence of fibrils up to 500-nm long and 20-nm wide (Figure 3a). These fibrils show a strong tendency to associate in a 3D network at higher concentrations. To examine the morphology of these fibrils in the gel state, freeze fracture electron microscopy (FFEM) experiments were performed, enabling preservation of the native structure of the gel and observation of the sample in the presence of nonane. Assemblies of short interconnected fibrils are clearly visible, but the crystallization of the solvent prevents the observation of the long-range orientation order of the fibrils.

To confirm that an aggregation process involving the fluorophore parts is at the origin of the sol/gel transition, optical measurements were used as analytical tools. A dilute solution of **1** in CH_2Cl_2 shows absorption typical of *F*-Bodipy derivatives with a strong peak ($S_0 \rightarrow S_1$ transition) at 525 nm, while in nonane this absorption is red-shifted (Figure S2). Furthermore, a typical intense green emission (at 540 nm) is found in CH_2Cl_2 , whereas a dual emission (at 537 and 576 nm) is found in nonane (Figure 4a). The emission band at 537 nm is assigned to the monomer, whereas the new red-shifted emission band at 576 nm is assigned to the formation of aggregates. As the concentration is lowered, the emission at 537 nm increases at the expense of the emission at 576 nm. The minimum concentration for aggregation is $6 \times 10^{-9} \text{ mol L}^{-1}$. These results are in line with the formation of molecular *J*-aggregates in which the excitonic energy is delocalized as a result of intermolecular coupling within the head-to-tail arrangement of the molecules.⁸ Monitoring the

luminescence as a function of temperature confirms that aggregation of the indacene core is the main driving force in gel formation.

The emission spectrum obtained from gels of nonane at $35 \text{ }^\circ\text{C}$ displayed an additional emission band at 592 nm. Upon heating, below the sol/gel transition at $48.5 \text{ }^\circ\text{C}$ as detected by DSC, no major modification of the three emission bands at 544, 576, and 592 nm were observed (Figure 4b). Nevertheless, above the sol/gel transition temperature in the fluid phase, the emission at 592 nm vanished and the emission at 576 nm increased. The emission at 592 nm is a clear signature of gel formation and is attributed, considering the bathochromic shift, to the emission of larger aggregates. A second transition, which could not have been detected with all the previous temperature-dependent methods, was observed between 55 and $78 \text{ }^\circ\text{C}$ and is assigned to the dissociation of aggregated species, emitting at 576 nm, into the monomer emitting at 544 nm. Further increase of the temperature led to diminution of the monomer luminescence due to dynamic quenching processes. Both transitions observed are completely reversible upon cooling.

The key feature of the present molecular design is the fusion of a semirigid diacylamido aromatic unit with a highly luminescent indacene. The products have several outstanding features: (i) liquid crystal formation over a wide temperature range, (ii) alkane solvent gelification due to aggregation of the indacene units and amide hydrogen bonding, (iii) strong fluorescence in the gels and mesophases. Fluorescence-imaging microscopy, used as a tool to monitor LC–liquid transition in the present work, offers new prospects for developing understanding of the packing of fluorescent molecules in microsegregation processes.

Acknowledgment. This work was supported by the CNRS, ULP, and ECPM. Drs. D. Guillon, B. Donnio, B. Heinrich from the IPCMS and Drs. L. Charbonnière and G. Ulrich from the LCM are gratefully acknowledged for their helpful discussions and their collaboration in the full understanding of the present system. We are also indebted to Professor J. Harrowfield for his critical reading.

Supporting Information Available: Complete Experimental Section, including preparation and characterization of **1**, DSC traces of a gel in nonane (22 g L^{-1}), and absorption spectra. This material is available free of charge via the Internet at <http://pubs.acs.org>.

References

- (1) (a) Estroff, L. A.; Hamilton, A. D. *Chem. Rev.* **2004**, *104*, 1201. (b) Sangeetha, N. M.; Maitra, U. *Chem. Soc. Rev.* **2005**, *34*, 821. (c) de Jong, J. J. D.; Lucas, L. N.; Kellogg, R. M.; van Esh, J. H.; Feringa, B. L. *Science* **2004**, *304*, 278. (d) Shirakawa, M.; Fujita, N.; Tani, T.; Kaneko, K.; Shinkai, S. *Chem. Commun.* **2005**, 4149. (e) Kubo, W.; Kitamura, T.; Hanabusa, K.; Wada, Y.; Yanagida, S. *Chem. Commun.* **2002**, 374.
- (2) Recent examples: (a) Sessler, J. L.; Callaway, W. B.; Dudek, S. P.; Date, R. W.; Bruce, D. W. *Inorg. Chem.* **2004**, *43*, 6650. (b) Cardinaels, T.; Ramaekers, J.; Guillon, D.; Donnio, B.; Binnemans, K. *J. Am. Chem. Soc.* **2005**, *127*, 17602. (c) Xiao, S.; Myers, M.; Miao, Q.; Sanaur, S.; Pang, K.; Steigerwald, M. L.; Nuckolls, C. *Angew. Chem., Int. Ed.* **2005**, *44*, 7390. (d) Wu, J.; Li, J.; Kolb, U.; Müllen, K. *Chem. Commun.* **2006**, 48.
- (3) (a) Beck, J. B.; Rowan, S. J. *J. Am. Chem. Soc.* **2003**, *125*, 13922. (b) Kawano, S.-I.; Fujita, N.; Shinkai, S. *J. Am. Chem. Soc.* **2004**, *126*, 8592.
- (4) Lee, K. Y.; Mooney, D. J. *Chem. Rev.* **2001**, *101*, 1869.
- (5) Ziessel, R.; Pickaert, G.; Camerel, F.; Donnio, B.; Guillon, D.; Cesario, M.; Prange, T. *J. Am. Chem. Soc.* **2004**, *126*, 12403.
- (6) Burghart, A.; Kim, H.; Wech, M. B.; Thorenson, L. H.; Reibenspies, J.; Burgess, K. *J. Org. Chem.* **1999**, *64*, 7813.
- (7) (a) Kato, T.; Kutsuna, T.; Hanabusa, K.; Ukon, M. *Adv. Mater.* **1998**, *10*, 606. (b) Yoshikawa, I.; Li, J.; Sakata, Y.; Araki, K. *Angew. Chem., Int. Ed.* **2004**, *43*, 100.
- (8) (a) Chen, H.; Farahat, M. S.; Law, K. Y.; Whitten, D. G. *J. Am. Chem. Soc.* **1996**, *118*, 2584. (b) von Berlepsch, H.; Boettcher, C.; Quart, A.; Burger, C.; Daehne, S.; Kirtsen, S. *J. Phys. Chem. B* **2000**, *104*, 5255.

JA0606069